Available online at www.sciencedirect.com
ScienceDirect
Journal of the European Ceramic Society 31 (2011) 1695–1701
www.elsevier.com/locate/jeurceramsoc

Strength of aluminium titanate/mullite composites containing thermal stabilizers

Fidel H. Perera [a], Antonia Pajares [a], Juan J. Meléndez [b,*]

[a] Departamento de Ingeniería Mecánica, Energética y de los Materiales, Universidad de Extremadura, Avda. de Elvas, s/n, 06006 Badajoz, Spain
[b] Departamento de Física, Universidad de Extremadura, Avda. de Elvas, s/n, 06006 Badajoz, Spain

Received 10 December 2010; received in revised form 28 February 2011; accepted 7 March 2011
Available online 3 April 2011

Abstract

This work contains a study on the room temperature-fracture strength of three aluminium titanate-based materials containing mullite and different thermal stabilizers (namely Fe_2O_3 and MgO). The highest inert strength was reached by the material sintered without any stabilizer. The MgO-doped material had a comparable inert strength, but a significantly higher Weibull modulus. Finally, the Fe_2O_3-doped material showed the worst mechanical properties. In all cases, a critical load above which strength degraded was apparent. These behaviours have been analyzed in terms of the type of additives and the particular microstructures. Conclusions about the potential use of these materials are briefly stated.

Keywords: Al_2TiO_5; Mullite; Mechanical properties; Strength; Additives

1. Introduction

Ceramic materials based on aluminium titanate (Al_2TiO_5) exhibit low thermal conductivity and excellent thermal shock resistance, among other properties. These make them usable in automobile and glass industries, in metallurgy and, more generally, in applications where good thermal insulation is required.[1] The properties of Al_2TiO_5 are greatly influenced by two facts. On one hand, aluminium titanate is chemically unstable at temperatures below 800 °C, from which it decomposes into the parent oxides alumina and rutile. The stabilization of the compound makes necessary the use of thermal stabilizers, mainly SiO_2, Fe_2O_3 and MgO[2]; the latter form with Al_2TiO_5 the solid solutions $Al_{2(1-x)}Fe_{2x}TiO_5$ and $Al_{2(1-x)}Mg_xTi_{1+x}O_5$, respectively.[3,4]

On the other hand, the microstructure of (stabilized) aluminium titanate exhibits a severe microcracking. Microcracks appear under cooling from the sintering temperatures due to the sharp anisotropy of the thermal expansion tensor[5]; its components (referred to the crystal normal axes) are $\alpha_a = 10.9 \times 10^{-6}\,K^{-1}$, $\alpha_b = 20.5 \times 10^{-6}\,K^{-1}$ and $\alpha_c = -2.7 \times 10^{-6}\,K^{-1}$ between room temperature and 1273 K.[6] Microcracking appears provided that the grain size is above a critical value (typically 1–3 μm),[7,8] and it is responsible for the excellent thermal shock resistance of these materials, but also for their poor mechanical properties (in particular, very low inert strength). To minimise the characteristic microcracking, reinforcing oxide phases are commonly added during processing; these are mainly mullite ($Al_6Si_2O_{13}$), zirconia and/or alumina, and remain as secondary phases once the material is cooled. The presence of these secondary phases gives rise to duplex microstructures.[9,10]

Both factors (the presence of secondary phases and need of thermal stabilizers) may well alter the mechanical properties of Al_2TiO_5. For instance, the grain size of aluminium titanate ceramics containing secondary phases depends upon their concentration[11]; the creep and thermal expansion behaviours of this system have been shown to be affected by the presence of stabilizers as well.[9,12] However, to the authors' knowledge the effect of the additives on the fracture strength of aluminium titanate-based materials has never been put forth in a systematic way. In this work, a preliminary study on the mechanical strength of three aluminium titanate/mullite ceramics containing different types of thermal stabilizers is presented. The results

* Corresponding author. Tel.: +34 924 289 655; fax: +34 924 289 651.
E-mail address: melendez@unex.es (J.J. Meléndez).

0955-2219/$ – see front matter © 2011 Elsevier Ltd. All rights reserved.
doi:10.1016/j.jeurceramsoc.2011.03.012

show a dependence on the type of additives, and are analyzed in terms of their particular microstructures. Conclusions for the potential use of these ceramics are briefly stated.

2. Experimental

2.1. Materials

The three aluminium titanate materials studied here were supplied by Starck Ceramics GmbH & Co. (Rödental, Germany). The detailed processing route, including amount of additives and sintering temperatures, is a property of the supplying company. All the three were fabricated by reactive sintering of an equimolar mixture of Al_2O_3 and TiO_2 powders. The mixture was homogenized with organic binders by milling. In one case, the homogenization took place without adding additives to the starting powder mixture; the resulting material will be referred to as AT hereafter. For the other two materials, either MgO or Fe_2O_3 was added to the starting powders to stabilize the resulting microstructure; these materials will be labelled as Mg-AT and Fe-AT, respectively. In all cases, 10 wt.% mullite ($Al_6Si_2O_{13}$) was added to the powder mixture in this first stage. Subsequently, the green bodies were sintered in air. After sintering, the density of the three materials was 3.3 g cm^{-3} (~90% of the theoretical density).

2.2. Microstructural characterization and mechanical tests

The microstructure and fracture surfaces of the as-received and tested materials were studied by optical microscopy with Nomarsky illumination (OM, Nikon Epiphot 300, Japan) and by scanning electron microscopy (SEM, Hitachi S-3600N, Japan). Samples for SEM observations were cut, ground and polished with diamond paste down to 1 μm finish, and then thermally etched; the thermal etching was carried out at 1450 °C during 45 min for AT and Mg-AT materials, and at 1500 °C during 60 min for Fe-AT. From the SEM micrographs, the grain size of each sample and phase (taken as the equivalent planar diameter $d = (4A/\pi)^{1/2}$, with A the grain area) was estimated by averaging on a population including no less than 500 grains.

The fracture strength was measured by four-point bending tests. Specimens were cut as parallelepipeds of approximate dimensions 2.5 mm × 2 mm × 30 mm; the tensile face and adjacent sides of each sample were ground and polished down to 1 μm finish to remove pre-existing flaws. These faces were subsequently indented by WC spheres of 1.58 mm radius under loads ranging between 0 N and 1000 N; these Hertz indentations were carried out to introduce defects of controlled size in the testing samples to cause their fracture. In bending tests, these imprints were kept at the tensile side. Hertz indentations and four-point bending tests were performed in a universal testing machine Instron 4465 (Instron Corp., USA) coupled to a proper data acquisition and analysis software. An inner span of 10 mm and an outer span of 20 mm were used for the measurements; the crosshead speed was set to 0.5 mm min^{-1}. At least five samples were used for each testing condition. OM observations were performed on fracture surfaces; in a few cases, samples were observed from one side to reveal the possible damage mode underneath the contact.

3. Results

3.1. Microstructure of the as-received samples

The micrograph in Fig. 1a shows the microstructure of the as-received AT material. The grains of the main phase (labelled as "AT") are equiaxed, with an approximate size of 5 μm. Mullite grains (labelled as "m") are dispersed homogeneously all over

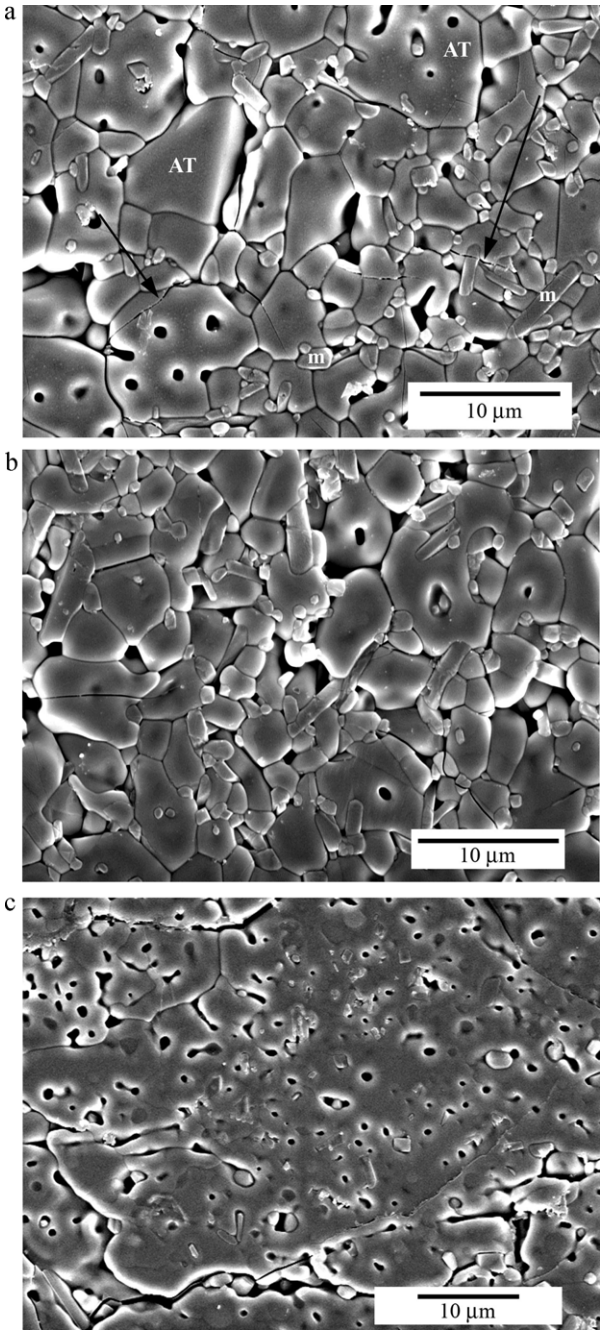

Fig. 1. SEM micrograph showing the microstructure of the AT (a), where the arrows point some characteristic microcracks, Mg-AT (b) and Fe-AT (c).

the sample, mainly located at contact points between several AT grains. They are mostly equiaxed, with an average size around 1 μm, although some acicular grains could also be seen. The observation of acicular mullite grains as well as the stabilization of the AT material (which did not contain any additive) suggest the presence of glassy SiO_2.[13] Porosity was also detected, either as cavities of relatively large size in triple points of the grain structure or as intragranular small pores less than 1 μm in size; both types of porosity are apparent in Fig. 1a.

Apart from these cavities or pores, the main flaws observed are the characteristic microcracks; some of them are indicated by arrows in Fig. 1a. The microcracks appear in either inter- or intragranular location, the former usually extending over several grains (either of the main phase or mullite). Microcracks seem to locate preferentially near nuclei of cavitation, with the cracks joining large-sized pores. These features are commonly observed in aluminium titanate ceramics with secondary phases.[11,12]

The morphologic characteristics of Mg-AT (Fig. 1b) are essentially analogous to those of AT. Two main differences arise however. Firstly, the grain size of the main phase is smaller (around 4 μm for Mg-AT). Secondly, the intergranular microcracks appear preferentially at the boundaries between similar grains (i.e., titanate–titanate or mullite–mullite). This fact may be associated with the presence of additives, since there is evidence suggesting that MgO increases the interfacial cohesion between the aluminium titanate and mullite phases.[14]

In opposition, the microstructure of Fe-AT is quantitatively different than the previous ones. Figs. 1c and 2 display SEM images of this material at different scales. Despite the thermal etching did not allow to reveal the grain boundaries (and, therefore, not to estimate the grain size of any phase either), it is reasonable to assume, according to what follows below, that this must be larger than that for AT. Anyway, the most important difference is that microcracks have a significantly larger size (which is evident in Fig. 2; note the different scale compared to Fig. 1a or b), to such an extent that they should no longer be considered as microscopic in a strict sense. These cracks also locate intra- and intergranularly, and their concentration is higher than in both AT and Mg-AT.

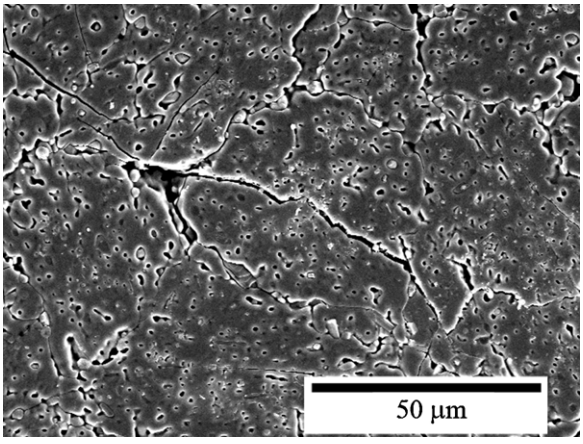

Fig. 2. SEM micrograph of Fe-AT at a lower magnification, note the relative size of the cracks compared to those shown in Fig. 1a or b.

3.2. Mechanical tests

Fig. 3a shows the fracture strength of AT as a function of the Hertzian indentation load applied to introduce defects. The inert strength of this material is 59 ± 9 MPa, and remains constant up to around 500 N. From that load on, the fracture strength decreases linearly with the indentation load up to 850 N; the transition is highlighted by a dashed line in the figure. Fig. 3b and c represent, respectively, the fracture strength vs. indentation load curves for Mg-AT and Fe-AT. These are qualitatively similar to

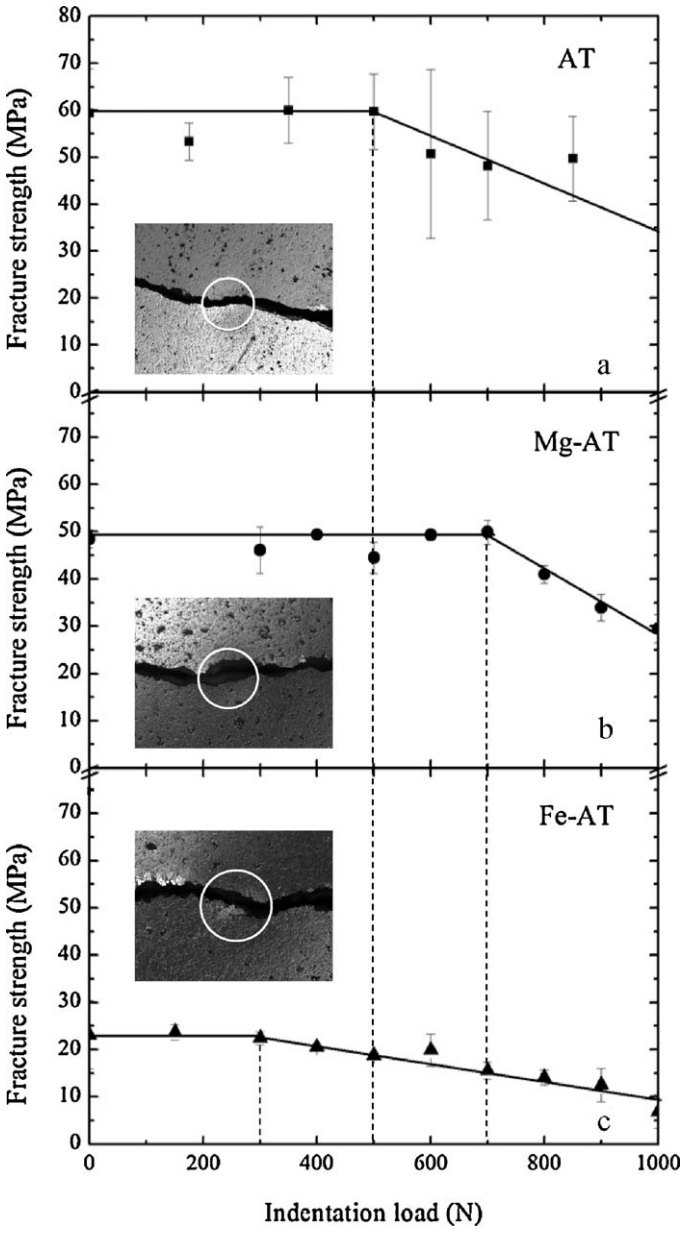

Fig. 3. Fracture strength vs. indentation load for AT (a), Fe-AT (b) and Mg-AT (c). The dashed lines depict the critical load for each material. The insets shows the top surfaces of failed samples previously indented under a 300 N load. The white circles fit approximately to the imprint of the Hertzian contact.

each other, and to that for AT. For Mg-AT, the inert strength is 49.4 ± 0.7 MPa up to an indentation load of around 700 N, from where it decreases linearly with the indentation load. For Fe-AT, the inert strength is significantly lower (23 ± 7 MPa), and remains constant up to an indentation load which is also lower than the previous (300 N); from this value on, the aforementioned lineal fall down is again observed. The dashed lines represent the proper transitions. The insets in Fig. 3a–c correspond to optical images of the top surfaces of failed samples indented with a 300 N load.

The fracture strength measured for each material under zero indentation load are within the range found in the literature for aluminium titanate ceramics with similar morphologic characteristics[15]; in all cases, the inert strengths are higher than that of the corresponding monolithic, no-reinforced, material (which is around 10 MPa[16] regardless the stabilizer), the difference being quite significant for AT and Mg-AT. The reinforcement of the materials is attributable to the presence of mullite.[11,15,16]

The observed trends can be put forth in an alternative way by means of the Weibull analysis. A material fails when a flaw grows uncontrolled after the stress intensity factor at the tip of the flaw reaches a critical value. Thus, failure requires the existence of a flaw of certain size conveniently located within the tensile region of the stress field: a flaw with these characteristics will be called a "proper flaw" hereafter. As a consequence, there is not a well-defined failure stress, but a failure stress distribution instead, because flaws of different sizes may be present within the tensile stress field. From a macroscopic point of view, the probability of failure under an applied stress σ may be accurately described by the so-called Weibull distribution,[17] namely:

$$P(\sigma) = 1 - \exp\left[\left(-\frac{\sigma}{\sigma_0}\right)^m\right] \quad (1)$$

where σ_0, the central value of the distribution, is a characteristic stress and m, the Weibull modulus, is a positive coefficient. The characteristic stress lacks of any precise physical meaning, but may be taken as an estimation of how high the inert strength is. The Weibull modulus provides pieces of information about the reliability of the material: the higher its value, the more reliable the material is (i.e., it has a narrower probability distribution).

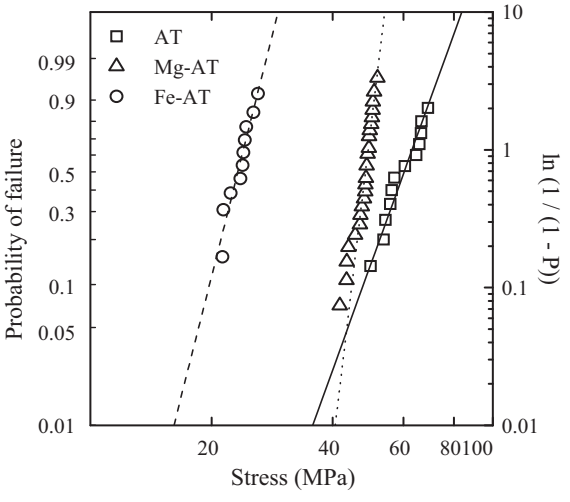

Fig. 4. Weibull plot for the materials considered in this study. According to Eq. (1), the log–log plot of $\ln(1/(1-P))$ vs. σ should yield a straight line with slope m and intercept $m \ln \sigma_0$, this quantity is plotted in the right axis. The left axis' scale is probabilistic.

Table 1
Results of the Weibull analysis for the three studied materials.

Material	σ_0 (MPa)	m
AT	60 ± 20	8.1 ± 0.5
Mg-AT	49 ± 15	24.4 ± 1.2
Fe-AT	24 ± 12	11.6 ± 1.2

Fig. 4 displays the inert strength vs. applied stress for unindented samples of the three materials. Each point corresponds to a four-point bending test performed on an unindented sample, and the straight lines are the best-fit ones of Eq. (1) to the experimental data. The respective central values and Weibull moduli are recorded in Table 1. According to these results, the most reliable material is Mg-AT which, however, exhibits an intermediate strength. Fe-AT has an intermediate Weibull modulus, and the characteristic value of the distribution is markedly lower than that for Mg-AT. Finally, the undoped AT material exhibits the highest strength, but also the minimum Weibull modulus.

3.3. Microstructural damage

The damage induced by the Hertzian contact was observed by OM. In a general sense, the damage pattern under Hertzian indentation may include cone cracks nucleated at the contact border, radial cracks generated underneath the contact and quasi-plastic damage below the contact under the surface of the sample[18]; the appearance of each damage mode depends on the macroscopic conditions as well as on microstructural features. In our case, there was no evidence of any kind of cone or radial cracks nearby the indentation imprint. There were instead clear signs of damage accumulation underneath the contact; this consisted essentially in the coalescence of cracks. The density and mean size of these were found to increase with the indentation load, so that it is reasonable to assume that some of them appeared under the action of the Hertzian stress field.

In addition, the analysis of the optical images revealed that failure of all the non-indented samples took place by the catastrophic growth of a proper crack located at an arbitrary position within the tensile field. For the indented samples, however, failure was caused always by the growth of proper cracks which crossed the indentation imprints.

The SEM micrograph in Fig. 5 shows the fracture surface of a non-indented AT sample. In this figure, the external faces of the grains (either of aluminium titanate or mullite phases) are clearly observed, which indicates that the fracture is intergranular in essence. The same conclusion may be stated for Mg-AT. The situation for Fe-AT is markedly different however. The SEM micrograph in Fig. 6 displays the fracture surface of a non-indented Fe-AT sample. In this case the external faces of the grains are not observed; on the contrary, the fracture surface is smooth, which indicates that the fracture is essentially

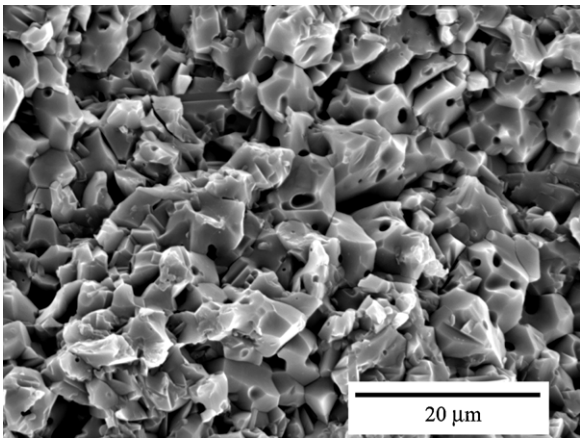

Fig. 5. SEM image of the fracture surface of an AT sample failed under zero load.

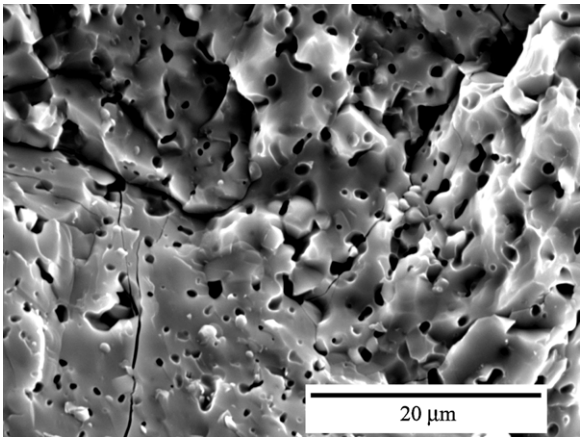

Fig. 6. SEM image of the fracture surface of a Fe-AT sample failed under zero load.

transgranular. This distinctive character is likely to be associated with the features of the cracking exhibited by this material (*cf.* Fig. 2).

4. Discussion

The analysis of the fracture mechanisms in materials with so complex chemical compositions and microstructures as those described here is a formidable task, all the more since some crucial details about the exact processing routes (such as the amount of additives) are unknown. Despite this, it is possible to state some semi-quantitative arguments in order to rationalize the experimental findings in terms of the type of additives and the particular microstructures.

Let us begin by analyzing the Weibull plot shown in Fig. 4 (or, equivalently, the data for zero indentation load in Fig. 3). According to this, the lowest and highest inert strengths are for Fe-AT and AT, respectively. In addition, we have stated above that failure is caused by the presence of relatively large flaws at regions where the stress field is intense enough (i.e., proper flaws). It seems then that the characteristic microcracking may well play some role. Several studies based on either energetic or mechanical criteria have allowed to derive a relationship between the critical grain size for the appearance of microcracking and the temperature difference which causes it.[19,20] In addition, Ohya and co-workers have obtained the following (empirical) relationship between the effective volume of microcracks V_{mic} and the grain size d in an aluminium titanate-based material[21]:

$$V_{mic} = 10^{0.16} \cdot d^{0.5} \tag{2}$$

where V_{mic} is expressed in percentage and d in microns. Eq. (2) remains valid regardless the type and amount of used additives, and also the amount of porosity existing in the materials. Eq. (2) relates the inert strength of the materials with the relative volume of microcracks. Indeed, the strength of a dense brittle material relates to its grain size as[22]:

$$\sigma_f = \sigma_{f0} \cdot d^{-r} \tag{3}$$

where σ_{f0} is a constant and $r>0$. In a general sense, the r value varies depending on the physical–chemical and morphological characteristics of each material. Taking into account Eq. (2), the relation between the fracture inert strength of an aluminium titanate-based material and the volume fraction of microcracks which it contains may be written as:

$$\sigma_f \propto V_{mic}^{-p} \tag{4}$$

with $p>0$. This conclusion is reasonable, since the higher the volume fraction of cracks, the higher also the probability to find a proper one at the tensile region of the stress field. In addition, it is in good agreement with the experimental findings, which show the order Fe-AT, Mg-AT and AT for the inert strength to increase, and with data reported elsewhere.[23]

A second argument may be argued which is based on the phenomenon of impurity segregation. Essentially, segregation in a ceramic alloy takes place when it contains impurities of ionic radius larger than that of the host atoms; in this case, the inclusion of dopants implies an elevated lattice distortion which may be relaxed through the expulsion of the dopant to a free surface, typically a grain boundary. When the impurities are aliovalent, there exists an additional contribution to the driving force for segregation which arises from the different effective electric charges of each species and that of the point defects generated to guarantee the electro-neutrality of the system.

In the case considered here, several studies have shown that the Al^{3+} and Ti^{4+} cations are disorderedly and equiprobably distributed within the cationic sublattice of Al_2TiO_5 regardless the thermal stabilizer employed.[17,18] On the other hand, in Fe_2O_3-doped materials, the Al^{3+} cations equimolarly substitute the Fe^{3+};[4] in MgO-doped ones, on their own, the corresponding substitution is $1\ Mg^{2+} + 1\ Ti^{4+} \rightarrow 2Al^{3+}$.[24] In both cases, a noticeable dissimilarity between the ionic radii of the host and dopant cations does exist; in particular, those for aluminium and titanium are, respectively, 0.50 Å and 0.68 Å, whereas those for iron and magnesium are 0.64 Å and 0.65 Å, respectively. In materials stabilized with iron and magnesium, the ratios between the ionic radii of the dopant and host cations are thus 1.28 and 1.33, respectively; in the YTZP system, where yttrium segregation has been widely reported, such a ratio is 1.16.[25] Accordingly, if further crystallographic or morphologic consid-

erations (like the dependence of segregation on the grain size and on the disorientation between grains, for instance) are neglected, it is reasonable to expect segregation to the grain boundaries in the aluminium titanate-based materials studied here. Studies devoted to detect it are in course; its presence could influence the different behaviours observed in our samples.

There exist some other parameters (not considered here), which may well affect the mechanical behaviour of the materials. The particular morphology of the grains (which is a key parameter when texture exists) or the shape of the grain size distribution could be relevant variables as well. Finally, the fracture strength is also highly influenced by the intensity of the interfacial joining at the grain boundaries.

The analysis of the complete curves displayed in Fig. 3 provides additional pieces of information. In all the cases, the strength exhibits the same trend: it remains constant up to a certain load which depends on the type of additive used, and it decreases monotonically from that load on. The observations suggest that this fall down is due to the damage accumulation as cracks coalesced underneath the Hertzian contact. Indeed, the higher the indentation load above the critical, the higher also the amount and size of potential proper flaws (coalescence is likely to proceed easier as the number of cracks increases), and therefore the probability of failure. The main difference between the three materials, apart from their particular inert strengths, is then the critical load after which the strength decreases. We think that this load could also be related to the size and relative volume fraction of pre-existing cracks. Thus, Fe-AT exhibits the lowest critical load because it already contains a high number of large cracks (i.e., a high number of potential proper cracks). In opposition, Mg-AT has the highest critical load probably due to the cohesive effect of MgO mentioned above.

The question remains as to the effect of the additives on the strength of our materials. This may be systematized, in the (simplified) schedule used here, attending to the amounts of microcracks to which they give rise. The very few bibliographical references to the effect of Fe_2O_3 on the microcraking of aluminium titanate show that this additive does not reduce significantly the amount of microcracks with respect to the undoped monolithic materials.[4] Fe-AT exhibits higher inert strength than monolithic AT because it contains mullite, but its volume fraction and size of microcracks is similar than those for monoliths, thence its much low strength and critical load for strength degradation.

For MgO-AT, there is evidence suggesting that MgO produces a light decrease in the amount of microcracks (or, alternatively, the grain size) in relation to undoped materials.[21] This is attributed to the formation of dislocations inherent to the solid solution Al_2TiO_5–$MgTi_2O_5$[26]; the existence of these dislocations provides an additional mechanism for stress relaxation during cooling from the sintering temperatures which reduces the amount of microcracks. It is then reasonable to think that the strength of an aluminium titanate ceramic stabilized with MgO should be comparable to (or even slightly higher than) the corresponding undoped material (provided that both of them contain mullite), also in relative agreement with the experimental results shown here. The fact that Mg-AT has the highest critical load for strength degradation could be related to the improved interfacial cohesion between aluminium titanate and mullite phases in the presence of MgO.[14] Thus, a higher load would be required for the critical crack density to be reached, which would justify the observed trend.

These assessments, although preliminary and somewhat simplified, are relevant in what relates to the potential uses of aluminium titanate ceramics. Indeed, in many of its applications not only thermal stability is required, but also appropriate mechanical properties which assure at least the integrity of the material under working conditions. In this sense, although both MgO and Fe_2O_3 are effective as thermal stabilizers, the room temperature mechanical properties of the corresponding aluminium titanate based materials may be drastically different. In particular, Fe_2O_3 should be avoided if mechanical resistance is required.

5. Conclusions

The experimental study presented here allows to justify that the fracture strength of aluminium titanate-based materials containing mullite as secondary phase is greatly influenced by the presence of additives. In all cases, mullite acts as a reinforcing phase, increasing the fracture strength with respect to the monolithic materials. MgO does not produce a significant change in the mechanical properties relative to the undoped material containing mullite; Fe_2O_3, in opposition, induces a severe microcracking of the samples which leads to a noticeable decrease of the fracture strength. These results have practical implications in situations where the mechanical integrity of stabilized aluminium titanate-based materials may be required.

References

1. Stingl P, Heinrich J, Huber J. Properties and application of aluminum titanate components. In: Bunk W, Hausner H, editors. *Proceedings of the 2nd International Symposium on ceramic materials and components for engines*. Bad Honnef: Lübeck-Travermünde; 1986. p. 369–80.
2. Hamano K, Nakagawa Z, Sawano K, Hasegawa M. Effects of additives on several properties of aluminium titanate ceramic. *Chem Soc Jpn* 1981;**10**:1647–55.
3. Buscaglia V, Nanni P, Battilana G, Aliprandi G, Carri C. Reaction sintering of aluminium titanate: I – the effect of MgO addition. *J Eur Ceram Soc* 1994;**13**:419–26.
4. Tilloca G. Thermal stabilization of aluminium titanate and properties of aluminium titanate solid solutions. *J Mater Sci* 1991;**26**:2809–14.
5. Bush EA, Hummel FA. High-temperature mechanical properties of ceramic materials: II. *J Am Ceram Soc* 1959;**48**:388–91.
6. Taylor D. Thermal-expansion data. 11. Complex oxides, A_2BO_5, and the garnets. *Brit Ceram Trans J* 1987;**86**:1–6.
7. Cleveland JJ, Bradt RC. Grain size microcracking relations for pseudobrookite oxides. *J Am Ceram Soc* 1978;**61**:478–81.
8. Ohya Y, Hamano K, Nakagawa Z. Microstructure and mechanical strength of aluminum titanate ceramics prepared from synthesized powders. *J Ceram Soc Jpn* 1983;**91**:289–97.
9. Lee HL, Jeong JY, Lee HM. Preparation of Al_2TiO_5 from alkoxides and the effects of additives on its properties. *J Mater Sci* 1997;**32**:5687–95.
10. Zhien L, Qingmin Z, Jianjun Y. The effects of additives on the properties and structure of hot-pressed aluminium titanate ceramics. *J Mater Sci* 1996;**31**:90–4.

11. Huang YX, Senos AMR, Baptista JL. Thermal and mechanical properties of aluminum titanate–mullite composites. *J Mater Res* 2000;**15**:357–63.
12. Meléndez-Martínez JJ, Jiménez-Melendo M, Domínguez-Rodríguez A, Wötting G. High-temperature mechanical behavior of aluminium titanate–mullite composites. *J Eur Ceram Soc* 2001;**21**:63–70.
13. Pask JA, Zhang XW, Tomsia AP, Yoldas BE. Effect of sol–gel mixing on mullite microstructure and phase-equilibria in the alpha-Al_2O_3–SiO_2 system. *J Am Ceram Soc* 1987;**70**:704–7.
14. Huang YX. *Doctoral thesis*. University of Aveiro, Portugal; 1998.
15. Huang YX, Senos AMR, Baptista JL. Preparation of an aluminium titanate–25 vol% mullite composite by sintering of gel-coated powders. *J Eur Ceram Soc* 1997;**17**:1239–46.
16. Ananthakumar S, Jayasankar M, Warrier KGK. Structural, mechanical and thermal characterisation of sol–gel-derived aluminium titanate–mullite ceramic composites. *Acta Mater* 2006;**54**:2965–73.
17. Weibull W. A statistical theory of the strength of materials. *Ing Vetenskaps Akad Handl* 1939;**151**:1–45.
18. Lawn BR. Indentation of ceramics with spheres: A century after Hertz. *J Am Ceram Soc* 1998;**81**:1977–94.
19. Ohya Y, Nakagawa Z, Hamano K. Grain-boundary microcracking due to thermal-expansion anisotropy in aluminum titanate ceramics. *J Am Ceram Soc* 1987;**70**:C184–6.
20. Davidge RW. Cracking at grain-boundaries in polycrystalline brittle materials. *Acta Metall* 1981;**29**:1695–702.
21. Ohya Y, Nakagawa Z. Measurement of crack volume due to thermal expansion anisotropy in aluminium titanate ceramics. *J Mater Sci* 1996;**31**:1555–9.
22. Kirchner HP, Gruver RM. Strength-anisotropy-grain size relations in ceramic oxides. *J Am Ceram Soc* 1970;**53**:232–6.
23. Huang YX, Senos AMR, Baptista JL. Engineering properties of aluminium titanate–mullite composites prepared by a gel coating process. *Silic Indus* 1998;**63**:51–6.
24. Ishitsuka M, Sato T, Endo T, Shimada M. Synthesis and thermal-stability of aluminum titanate solid-solutions. *J Am Ceram Soc* 1987;**70**:69–71.
25. Gómez-García D, Lorenzo-Martín C, Muñoz-Bernabé A, Domínguez-Rodríguez A. Correlation between yttrium segregation at the grain boundaries and the threshold stress for plasticity in yttria-stabilized tetragonal zirconia polycrystals. *Philos Mag* 2003;**83**:93–108.
26. Ohya Y, Hamano K, Nakagawa Z. Effects of some additives on microstructure and bending strength of aluminum titanate ceramics. *J Ceram Soc Jpn* 1986;**94**:665–70.